

## Differential Measurement of Electron Ejection after Two-Photon Two-Electron Excitation of Helium

Michael Straub<sup>1</sup>, Thomas Ding<sup>1</sup>, Marc Rebholz<sup>1</sup>, Gergana D. Borisova<sup>1</sup>, Alexander Magunia<sup>1</sup>, Hannes Lindenblatt<sup>1</sup>, Severin Meister<sup>1</sup>, Florian Trost<sup>1</sup>, Yimeng Wang<sup>2</sup>, Steffen Palutke<sup>3</sup>, Markus Braune<sup>3</sup>, Stefan Düsterer<sup>3</sup>, Rolf Treusch<sup>3</sup>, Chris H. Greene<sup>2</sup>, Robert Moshhammer<sup>1,‡</sup>, Thomas Pfeifer<sup>1,†</sup> and Christian Ott<sup>1,\*</sup>

<sup>1</sup>Max-Planck-Institut für Kernphysik, Saupfercheckweg 1, D-69117 Heidelberg, Germany

<sup>2</sup>Department of Physics and Astronomy, Purdue University, West Lafayette, Indiana 47907, USA

<sup>3</sup>Deutsches Elektronen Synchrotron DESY, Notkestrasse 85, D-22607 Hamburg, Germany



(Received 3 June 2022; accepted 4 October 2022; published 28 October 2022)

We report the measurement of the photoelectron angular distribution of two-photon single-ionization near the  $2p^2\ ^1D^o$  double-excitation resonance in helium, benchmarking the fundamental nonlinear interaction of two photons with two correlated electrons. This observation is enabled by the unique combination of intense extreme ultraviolet pulses, delivered at the high-repetition-rate free-electron laser in Hamburg (FLASH), ionizing a jet of cryogenically cooled helium atoms in a reaction microscope. The spectral structure of the intense self-amplified spontaneous emission free-electron laser pulses has been resolved on a single-shot level to allow for post selection of pulses, leading to an enhanced spectral resolution, and introducing a new experimental method. The measured angular distribution is directly compared to state-of-the-art theory based on multichannel quantum defect theory and the streamlined  $R$ -matrix method. These results and experimental methodology open a promising route for exploring fundamental interactions of few photons with few electrons in general.

DOI: [10.1103/PhysRevLett.129.183204](https://doi.org/10.1103/PhysRevLett.129.183204)

The reaction of few photons with few electrons is a fundamental process of nonlinear light-matter interaction at high laser intensities. The helium atom, with its two bound electrons represents an important benchmark system for the quantum description of two correlated electrons [1,2] and their response to intense radiation fields [3]. At energies  $\sim 60$  eV above the ground state, and still below the double-ionization threshold at 79 eV, autoionizing states are a direct manifestation of electron correlation. Besides the energy-dependent ionization yield, governed by the cross section, the measurement of the photoelectron angular distribution provides a comprehensive insight into the correlated electron-electron interaction of the involved autoionizing states, specifically when two photons are absorbed [4,5].

With the advent of short-wavelength free-electron lasers (FELs) [6,7] the nonlinear interaction of helium with intense extreme ultraviolet (XUV) radiation became experimentally possible [8,9]. Measured through spectroscopy with the tunable seeded FEL FERMI, the two-photon

excitation of dipole-forbidden autoionizing states in helium and their energy shifts have been observed [10]. The modification of autoionizing states in intense radiation fields at  $\sim 60$  eV has also been observed through a change in the measured Fano absorption line shape [11]. The photoelectron angular distribution after two-photon single ionization of helium has been reported and discussed both experimentally and theoretically [12–15], drawing attention to the role of both resonant and nonresonant interaction pathways with a single active electron.

In this Letter we report on the differential measurement of the photoelectron angular distribution (PAD) of two-photon single ionization (TPSI) in helium, involving a transient double excitation near the final (continuum) state. To distinguish nonlinear ionization events from a large one-photon ionization background, we use the event-based detection scheme of a cold-target recoil-ion momentum spectroscopy reaction microscope (REMI) [16], providing high momentum resolution by means of a cryogenically cooled supersonic jet of helium atoms. The REMI detection of the TPSI PAD is combined with a high-resolution photon spectrometer to measure, individually for each FEL pulse, the incoming FEL spectral intensity distribution. Resolving the typically structured self-amplified spontaneous emission (SASE) FEL spectra allows one to improve the spectral resolution [17] in a similar way as ghost imaging [18]. Here we further develop this methodology in the nonlinear case, extracting weak nonlinear ionization signals

Published by the American Physical Society under the terms of the [Creative Commons Attribution 4.0 International](https://creativecommons.org/licenses/by/4.0/) license. Further distribution of this work must maintain attribution to the author(s) and the published article's title, journal citation, and DOI. Open access publication funded by the Max Planck Society.

from a much larger background of linear ionization events. Thereby we apply a new experimental methodology to make an essential step in improving our fundamental understanding of nonlinear light-matter interaction involving two active and correlated electrons.

The experiment was performed at the free-electron laser in Hamburg (FLASH), at the REMI endstation at the FLASH2 beamline FL26 [19], where we have recently installed a high-resolution XUV photon spectrometer for transient absorption spectroscopy. The experimental setup is illustrated in Fig. 1(a). The linearly polarized (along the  $y$  direction) FEL pulses at 30 eV photon energy are delivered with an effective 540 Hz repetition rate in 10 Hz burst mode (54 pulses with 10  $\mu$ s spacing) with a mean pulse energy of a few  $\mu$ J, as determined by a gas monitor detector upstream of the experimental setup. The FEL beam is focused (spot size  $\sim 10$   $\mu$ m) into the center of the REMI, crossing a supersonic jet of cryogenically cooled helium atoms. The produced ions are guided by a homogeneous electric field onto a time- and position-sensitive multichannel-plate detector with delay-line anode. This detection scheme allows one to reconstruct the three-dimensional momentum of  $\text{He}^+$  for each photoionization event. After transmission through the REMI, the SASE spectral intensity distribution of each FEL pulse is measured with a grating-based high-resolution XUV photon spectrometer. The spectrometer is equipped with a high-repetition rate GOTTHARD detector [20] to resolve individual pulses within one burst as in Ref. [17]. An ensemble of XUV spectra from 54 consecutive FEL pulses within one burst is depicted in Fig. 1(a) on the right. The energy resolution of the XUV photon spectrometer was determined via a calibration measurement of the argon 3s autoionizing resonances [21], yielding 30 meV at 28.0 eV.

Because of momentum conservation, neglecting the photon momentum  $|\vec{p}_\gamma| < 0.01$  a.u., the photoelectron momentum  $|\vec{p}_e| \gtrsim 1$  a.u. is fully reflected by the recoil momentum of the helium ion  $\vec{p}_{\text{He}^+}$ , with  $\vec{p}_e = -\vec{p}_{\text{He}^+}$ . Hence the PAD can be inferred from the measured  $\vec{p}_{\text{He}^+}$  recoil-ion momentum distribution. A slice of the  $\text{He}^+$  momentum distribution in the  $x$ - $y$  plane ( $|p_z| \leq 0.1$  a.u.) is depicted in Fig. 1(b). The incoming FEL beam predominantly singly ionizes helium with one photon, leading to a pronounced maximum at  $p_r \approx 0.6$  a.u. with its characteristic P-lobe angular distribution (angular momentum  $L = 1$ ), aligned along the FEL polarization direction, where  $p_r = \sqrt{p_x^2 + p_y^2}$  is the radial momentum in the  $x$ - $y$  plane. Benefitting from the cold and dilute jet of target atoms, the momentum resolution is sufficiently high to distinguish the weak nonlinear TPSI events appearing at  $p_r \approx 1.6$  a.u., where the selected region for further analysis is indicated by red circles.

The FEL photon energy was tuned to half the  $2p^2$   $1\text{D}^e$  autoionizing resonance at 59.9 eV [see level scheme in Fig. 2(a)], where the corresponding two-photon cross

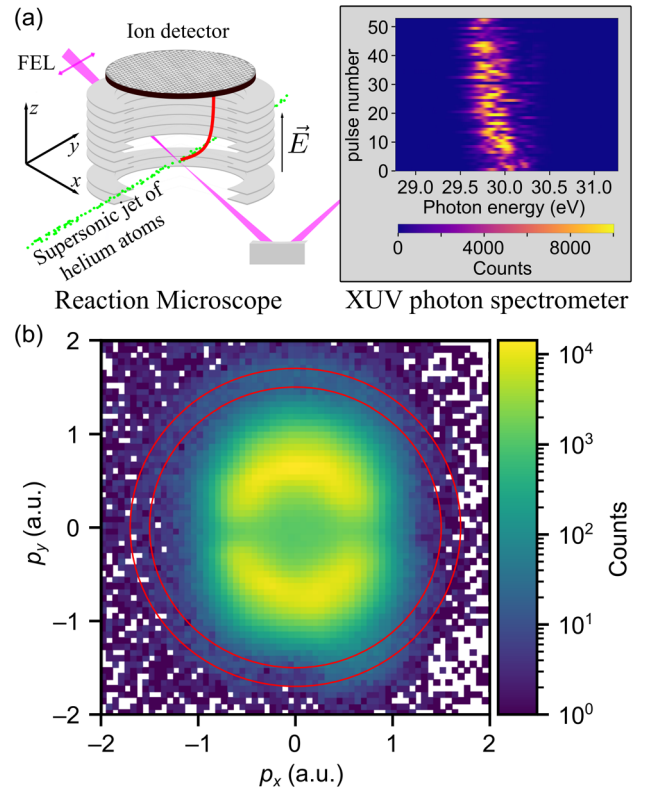


FIG. 1. (a) The experimental setup: Linearly polarized FEL pulses arrive from the left, propagating in the  $x$  direction, and are focused into the center of the reaction microscope, crossing a supersonic gas jet of cryogenically cooled atomic helium. The created ions are then accelerated toward a position- and time-sensitive detector. The transmitted FEL beam is refocused into a grating spectrometer, measuring the XUV photon spectrum on a shot-to-shot basis with the GOTTHARD detector [20], compatible with the burst-mode high-repetition rate pulse pattern at FLASH, similar to Ref. [17]. (b) The measured recoil-ion momentum distribution in the  $x$ - $y$  plane with a slice in the  $z$  direction ( $|p_z| \leq 0.1$  a.u.). The FEL is polarized in the  $y$  direction. Two-photon ionization events are selected by their momentum  $1.5 \text{ a.u.} \leq |\vec{p}_e| \leq 1.7 \text{ a.u.}$  as marked by the red circles. Because of a locally confined inhomogeneity in the detector efficiency at very negative  $p_y$  momenta, only events in the upper hemisphere ( $p_y \geq 0$ ) are considered for the analysis.

section [5] is plotted in Fig. 2(b). Sorting REMI photoionization events by the measured SASE FEL spectral intensity distribution allows for a finer photon-energy resolution to resolve the  $2p^2$   $1\text{D}^e$  resonance. The latter is much narrower than the FEL average spectral bandwidth of 430 meV at FWHM, as determined from the measured average spectra. In Fig. 3 (lower panel) the spectra are sorted by the photon-energy position of the highest peak for each single SASE spectrum, distributed into equidistant bins of  $\sim 31$  meV. To keep the number of photons per pulse approximately constant for each spectral bin, we restrict the pulse energy to between 4.2 and 4.7  $\mu$ J. These values result from casting all FEL shots of the run, whose pulse energy

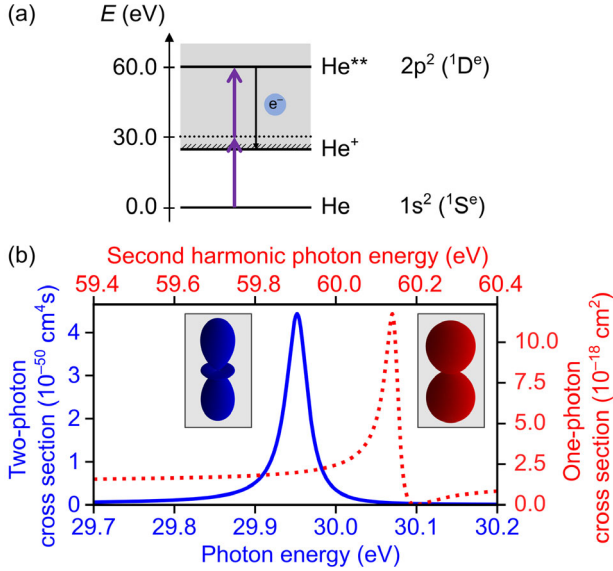


FIG. 2. (a) Energy level scheme of the observed ionization channel. The doubly excited state  $2p^2$  ( $^1D_e$ ) at 59.9 eV can be reached with two FEL photons (vertical purple arrows) tuned to half the transition energy. This state primarily decays through autoionization, emitting an electron (thin black arrow) into the He<sup>+</sup> ionization continuum. (b) Calculated total two-photon cross section in blue [5]. The blue inset shows the PAD at the peak of the cross section which features a dominant D symmetry. Additionally, the calculated one-photon cross section is shown (red, dashed) at twice the photon energy [22,23]. The red inset shows the corresponding one-photon  $P$  lobe.

ranges from almost zero up to above  $\sim 5$   $\mu\text{J}$  due to the SASE-FEL mode of operation, into a distribution of nine pulse-energy bins, while keeping a constant number of FEL pulses per bin. We then select the second highest pulse-energy bin, excluding outliers in the high-pulse-energy tail of the SASE distribution. This effectively creates a narrow-band photon-energy sweep with a resolution better than 0.1 eV that can now be applied to the shot-by-shot recorded photoionization events of the REMI.

The absorption of two  $\sim 30$  eV photons leads to the emission of a fast photoelectron with  $|\vec{p}_e| \approx 1.6$  a.u. With the condition  $1.5 \text{ a.u.} \leq |\vec{p}_e| \leq 1.7 \text{ a.u.}$  [cf. red circles in Fig. 1(b)], the number of events is determined separately for each bin of the previously described energy sweep and normalized by the number of pulses in that bin. The result is plotted in blue color in the upper panel of Fig. 3. It exhibits a maximum at 29.95 eV, corresponding to the  $2p^2$   $^1D_e$  autoionizing resonance [cf. Fig. 2(b)]. Furthermore we observe a shoulder extending to higher photon energy, which we attribute to direct one-photon ionization by the second harmonic of the FEL, enhanced by the resonant cross section as depicted by the dashed red line in Fig. 2(b). Assuming 1% of the fundamental photon flux in the second harmonic, with the fundamental intensity on the order of  $10^{13}$  W/cm<sup>2</sup>, the theoretically calculated one-photon and

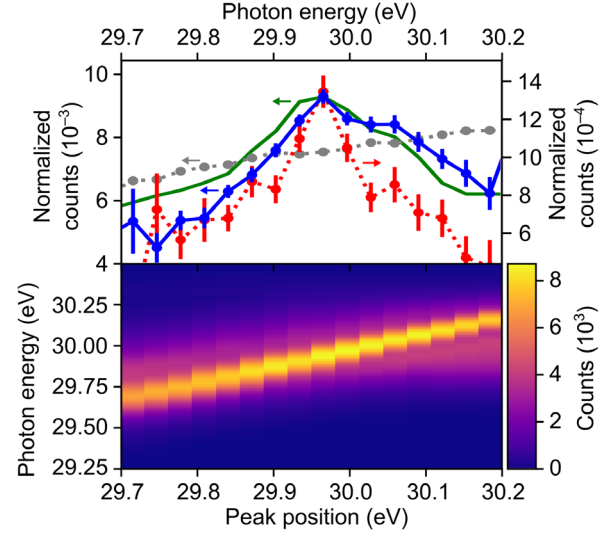


FIG. 3. Lower panel: mean FEL spectra sorted by the photon-energy position of the highest peak in each SASE spectrum, where the pulse energy is restricted to values between 4.2 and 4.7  $\mu\text{J}$ . Upper panel: the blue data depict the relative counts of a fast recoil ion ( $1.5 \text{ a.u.} \leq |\vec{p}_e| \leq 1.7 \text{ a.u.}$ ), normalized to the number of pulses in each bin. The gray data show the relative counts (scaled by  $10^{-2}$ ) of direct one-photon ionization events ( $|\vec{p}_e| \approx 0.6 \text{ a.u.}$ ) for each bin. The green curve is obtained by convoluting the experimental FEL spectra with the theoretical cross section [cf. Fig. 2(b)], assuming a 1% photon flux of the second harmonic compared to the fundamental. The red data are obtained by selecting fast recoil ions ( $1.5 \text{ a.u.} \leq |\vec{p}_e| \leq 1.7 \text{ a.u.}$ ) with the additional condition of a small momentum in the polarization direction ( $|p_y| \leq 0.3 \text{ a.u.}$ ).

two-photon cross section [cf. Fig. 2(b)] is convoluted with the experimentally measured average FEL spectra per bin (cf. Fig. 3, lower panel). The photon flux of the second harmonic has been estimated with an uncertainty on the order of 50% by the measured count rate of helium ions with an attenuated FEL beam, efficiently suppressing the TPSI nonlinear contribution. Furthermore we assume the second harmonic FEL spectrum is a copy of the measured fundamental spectrum at twice the photon energy. This results in the green curve depicted in the upper panel of Fig. 3, which qualitatively agrees with the experimental data. For further confirmation, we evaluate the relative probability of the direct one-photon ionization events at  $|\vec{p}_e| \approx 0.6$  a.u., sorted in the same manner by the SASE spectral peak positions, where the result is plotted in gray color in the upper panel of Fig. 3. Because of the lack of any resonances in this region, a smooth and featureless trend is observed. To further isolate the nonlinear TPSI of helium and suppress the linear background of the FEL second harmonic, we can make use of angular momentum conservation. The second harmonic photoemission with angular momentum  $L = 1$  is forbidden in the direction perpendicular to the FEL polarization axis, i.e., for  $p_y = 0$ . We thus set the additional condition of a low

momentum component along the polarization direction (i.e.,  $|p_y| \leq 0.3$  a.u.), where the accordingly reduced counts are depicted in red color in Fig. 3. As a result, the peak at 29.95 eV, corresponding to the  $2p^2 \ ^1D^e$  two-photon resonance, is now even sharper and appears more symmetric, while the shoulder at 30.05 eV, corresponding to an enhancement of the one-photon ionization with the FEL second harmonic, is now efficiently suppressed.

Having identified the signature of the  $2p^2 \ ^1D^e$  doubly excited state in the experiment we now turn to extracting the PAD at the peak of this resonance. Selecting the centermost (i.e., resonant) spectral bins of Fig. 3 alone does not provide enough statistics for a differential analysis of the corresponding angular distribution. We thus further improve the sorting of SASE spectra that lead to resonantly enhanced TPSI of helium with a new classification scheme. Hereby we apply a narrow spectral window from 29.9 to 30.0 eV on the measured XUV spectrum of each FEL pulse, for which we also measure a fast  $\text{He}^+$  recoil ion in the REMI. The integrated spectrum in this 0.1 eV window is normalized by the integrated total spectrum, yielding for each pulse the relative spectral intensity at the resonant XUV photon energy. The FEL pulses are accordingly sorted by this relative spectral intensity into a distribution of three bins with an equal number of pulses per bin. The highest and lowest bin we hereafter classify as resonant and off-resonant datasets. The accumulated FEL spectra for these two cases are plotted in Fig. 4(a), where in the following we now analyze the corresponding angular distributions measured in coincidence with the REMI.

The PAD of fast helium recoil ions ( $1.5 \text{ a.u.} \leq |\vec{p}_e| \leq 1.7 \text{ a.u.}$ ) for both the resonant and off-resonant case is depicted in Fig. 4(b). The off-resonant counts have been renormalized by the ratio of the total number of incoming photons for both PADs, as determined from the integrated spectral intensity distributions shown in Fig. 4(a). Considering the resonant case in Fig. 4(b), we observe a local maximum for the electron emission angle at  $90^\circ$ , which is expected for a dominant contribution of the  $2p^2 \ ^1D^e$  resonance with total angular momentum  $L = 2$  [cf. Fig. 2(b)]. In contrast, for the off-resonant case, the yield at  $90^\circ$  shows a reduced local maximum, and the overall shape more resembles that of a p wave [total angular momentum  $L = 1$ , cf. Fig. 2(b)], with a reduced d-wave content. A more dominant p wave is expected for one-photon ionization of helium with the second harmonic of the FEL. This observation is in agreement with the discussion of Fig. 3, where a background of fast recoil ions from ionization with the second harmonic of the FEL has been identified.

In order to quantitatively compare the experimental PAD to theory, in a first attempt we assume the renormalized off-resonant PAD as a simple background, and hence subtract it from the resonant PAD, resulting in the angular distribution of counts shown in Fig. 4(c). The PAD for two-photon

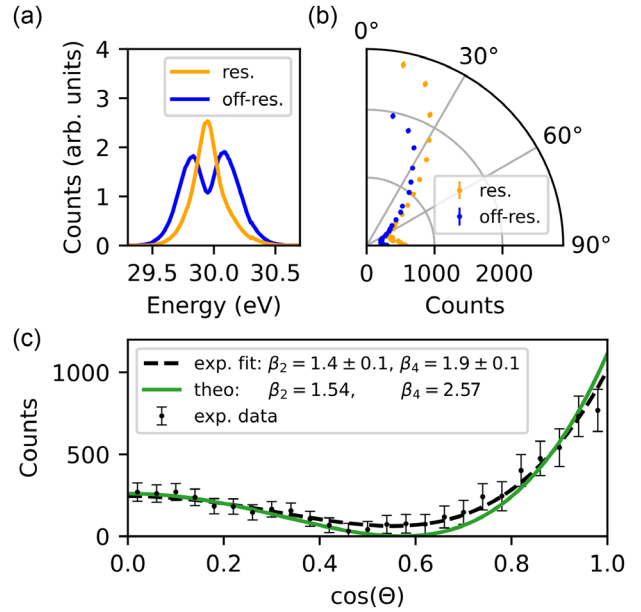


FIG. 4. (a) Accumulated FEL spectra, measured with the XUV photon spectrometer, for high (orange) and low (blue) relative photon flux on resonance, i.e., between 29.9 to 30.0 eV. (b) PAD of fast recoil ions ( $1.5 \text{ a.u.} \leq |\vec{p}_e| \leq 1.7 \text{ a.u.}$ ), measured with the REMI, and accumulated for the condition of FEL spectra with resonant (orange) and off-resonant (blue) pulses, resulting from the corresponding FEL spectra which are plotted in (a). The counts of the off-resonant case have been renormalized by the ratio of the total number of incoming photons for both cases. (c) Subtracting the measured background (renormalized off-resonant counts) from the signal (resonant counts) from (b) isolates the PAD of the two-photon double-excitation resonance shown in (c). The dashed black line depicts the least-squares fit to the experimental data, together with the best fit parameters and statistical error bars given by the standard deviation. The solid green line denotes the theory prediction at the peak of the resonance with given  $\beta_2$  and  $\beta_4$  parameters.

ionization can be described by using a sum of even-rank Legendre polynomials  $P_k(\cos \theta)$  up to fourth order and asymmetry parameters  $\beta_k$ , where  $\theta$  is the angle of the measured momentum direction with respect to the laser polarization direction, which is aligned along the y axis. Together with the total cross section  $\sigma_0$ , the PAD can be expressed through

$$\frac{d\sigma}{d\Omega} = \frac{\sigma_0}{4\pi} [1 + \beta_2 P_2(\cos \theta) + \beta_4 P_4(\cos \theta)]. \quad (1)$$

The resulting fit and its  $\beta_2$  and  $\beta_4$  parameters are shown in Fig. 4(c) and can be directly compared to theory, where the angular distribution is extracted at the maximum of the two-photon cross section [cf. Fig. 2(b)]. The theoretical two-photon ionization amplitudes utilized in the present study were obtained in the previous study, Ref. [5]. In Fig. 4 of that reference, the accuracy is confirmed by the excellent agreement with the total cross sections and asymmetry that

were determined in this energy range in the time-dependent calculations of Boll *et al.*, in Ref. [4]. The general trend of the theoretical distribution is well captured by the experiment; however a significant discrepancy beyond the statistical uncertainty remains. We have ascertained that both a finite angular resolution of the measurement, as well as averaging over a finite energy window across the resonance can be neglected on the stated results. Both contributions range within the same order as given by the statistical error bars of the extracted  $\beta_{2,4}$  parameters. Assuming a  $\pm 10\%$  systematic uncertainty for the renormalization of the off-resonant PAD counts yields a systematic shift of the fitted  $\beta_2$  and  $\beta_4$  parameters, respectively, by  $^{+0.1}_{-0.2}$  and  $^{-0.2}_{+0.4}$ . Because of the shifts of the  $\beta_{2,4}$  parameters in different directions, the systematic contribution of a scaled background thus also cannot fully explain the deviation to theory. It seems likely that the actual FEL pulse shapes, with their partially coherent spectrotemporal SASE structure, have to be considered. Concerning the modeling for an *ab initio* theory of correlated two-electron dynamics in helium, the extension to both high intensity and a typical average pulse duration on the order of 100 fs still poses a major challenge, which goes beyond the scope of the current work. Both of which are however important, with SASE FEL pulses containing temporal spikes well above the average intensity level, which are stochastically distributed over the average pulse duration [24,25], and which play a crucial role especially when resonant transitions are involved [11]. Furthermore, concerning the FEL second harmonic, theory predicts interfering pathways for the coherent interaction between one- and two-photon pathways in this energy region [26]. In the Supplemental Material [27] we identify a heterodyne effect through the coherent interaction between the fundamental and second harmonic. After averaging their relative phase over a full  $2\pi$  range, which is compatible with the experiment where we expect the relative phase to fluctuate from shot to shot, the calculated PAD is significantly changed, approaching the experimental one. Coherent interactions may thus be a likely explanation for the remaining discrepancy between theory and experiment for the reported differential measurement of the photoelectron angular distribution. This creates an exciting prospect, triggering new experiments and theoretical modeling for the exploration of novel coherent-control schemes with SASE FEL pulses.

In conclusion, we have experimentally resolved the nonlinear interaction of two photons with two correlated electrons in helium in the vicinity of the  $2p^2\ ^1D^e$  auto-ionizing resonance. The yield of photoionization was measured differentially as a function of photon energy and the photoelectron emission angle, and compared to theory. The experiment was enabled by the unique combination of measuring high-resolution recoil-ion momenta with a cryogenically cooled target in the REMI together with synchronous recording of the incident FEL spectra on

a shot-to-shot basis. This scheme has been crucial to identify small yields of nonlinear two-photon processes in the presence of high count rates of linear events from one-photon ionization. The spectrally broad SASE FEL pulses in combination with single-pulse selected spectra allowed for a simultaneous photon-energy sweep in the experimental analysis with substantially improved resolution. This scheme relates to and possibly extends other spectral-domain ghost-imaging approaches [28] now into the regime of nonlinear light-matter interaction.

We acknowledge DESY (Hamburg, Germany), a member of the Helmholtz Association HGF, for the provision of experimental facilities as well as for the Maxwell computational resources. Parts of this research were carried out at FLASH, and we would like to thank its technical and scientific teams for assistance in the preparation of and during the beamtime at the REMI at beamline FL26, which was allocated for proposal F-20181217. For their technical support, we thankfully acknowledge Christian Kaiser and Alexander von der Dellen, as well as the in-house technical workshops at MPIK. The work of Yimeng Wang and Chris H. Greene was supported by the U.S. Department of Energy, Office of Science, Basic Energy Sciences, under Award No. DESC0010545.

---

\*christian.ott@mpi-hd.mpg.de

†thomas.pfeifer@mpi-hd.mpg.de

‡r.moshhammer@mpi-hd.mpg.de

- [1] U. Fano, Correlations of two excited electrons, *Rep. Prog. Phys.* **46**, 97 (1983).
- [2] G. Tanner, K. Richter, and J.-M. Rost, The theory of two-electron atoms: Between ground state and complete fragmentation, *Rev. Mod. Phys.* **72**, 497 (2000).
- [3] P. Lambropoulos, P. Maragakis, and J. Zhang, Two-electron atoms in strong fields, *Phys. Rep.* **305**, 203 (1998).
- [4] D. I. R. Boll, O. A. Fojón, C. W. McCurdy, and A. Palacios, Angularly resolved two-photon above-threshold ionization of helium, *Phys. Rev. A* **99**, 023416 (2019).
- [5] Y. Wang and C. H. Greene, Two-photon above-threshold ionization of helium, *Phys. Rev. A* **103**, 033103 (2021).
- [6] W. Ackermann *et al.*, Operation of a free-electron laser from the extreme ultraviolet to the water window, *Nat. Photonics* **1**, 336 (2007).
- [7] S. Schreiber and B. Faatz, The free-electron laser FLASH, *High Power Laser Sci. Eng.* **3**, e20 (2015).
- [8] A. A. Sorokin, S. V. Bobashev, T. Feigl, K. Tiedtke, H. Wabnitz, and M. Richter, Photoelectric Effect at Ultra-high Intensities, *Phys. Rev. Lett.* **99**, 213002 (2007).
- [9] M. Kurka *et al.*, Differential cross sections for non-sequential double ionization of He by 52 eV photons from the Free Electron Laser in Hamburg, FLASH, *New J. Phys.* **12**, 073035 (2010).
- [10] M. Žitnik *et al.*, High Resolution Multiphoton Spectroscopy by a Tunable Free-Electron-Laser Light, *Phys. Rev. Lett.* **113**, 193201 (2014).

- [11] C. Ott *et al.*, Strong-Field Extreme-Ultraviolet Dressing of Atomic Double Excitation, *Phys. Rev. Lett.* **123**, 163201 (2019).
- [12] R. Moshhammer *et al.*, Second-order autocorrelation of XUV FEL pulses via time resolved two-photon single ionization of He, *Opt. Express* **19**, 21698 (2011).
- [13] K. L. Ishikawa and K. Ueda, Competition of Resonant and Nonresonant Paths in Resonance-Enhanced Two-Photon Single Ionization of He by an Ultrashort Extreme-Ultraviolet Pulse, *Phys. Rev. Lett.* **108**, 033003 (2012).
- [14] R. Ma *et al.*, Photoelectron angular distributions for the two-photon ionization of helium by ultrashort extreme ultraviolet free-electron laser pulses, *J. Phys. B* **46**, 164018 (2013).
- [15] K. L. Ishikawa and K. Ueda, Photoelectron angular distribution and phase in two-photon single ionization of H and He by a femtosecond and attosecond extreme-ultraviolet pulse, *Appl. Sci.* **3**, 189 (2013).
- [16] J. Ullrich, R. Moshhammer, A. Dorn, R. Dörner, L. Ph. H. Schmidt, and H. Schmidt-Böcking, Recoil-ion and electron momentum spectroscopy: Reaction-microscopes, *Rep. Prog. Phys.* **66**, 1463 (2003).
- [17] S. Palutke, N. C. Gerken, K. Mertens, S. Klumpp, A. Mozzanica, B. Schmitt, C. Wunderer, H. Graafsma, K.-H. Meiwes-Broer, W. Wurth, and M. Martins, Spectrometer for shot-to-shot photon energy characterization in the multi-bunch mode of the free electron laser at Hamburg, *Rev. Sci. Instrum.* **86**, 113107 (2015).
- [18] T. Driver *et al.*, Attosecond transient absorption spectroscopy: A ghost imaging approach to ultrafast absorption spectroscopy, *Phys. Chem. Chem. Phys.* **22**, 2704 (2020).
- [19] G. Schmid, K. Schnorr, S. Augustin, S. Meister, H. Lindenblatt, F. Trost, Y. Liu, M. Braune, R. Treusch, C. D. Schröter, T. Pfeifer, and R. Moshhammer, Reaction microscope endstation at FLASH2, *J. Synchrotron Radiat.* **26**, 854 (2019).
- [20] A. Mozzanica, A. Bergamaschi, R. Dinapoli, H. Graafsma, D. Greiffenberg, B. Henrich, I. Johnson, M. Lohmann, R. Valeria, B. Schmitt, and S. Xintian, The GOTTHARD charge integrating readout detector: Design and characterization, *J. Instrum.* **7**, C01019 (2012).
- [21] S. L. Sorensen, T. Åberg, J. Tulkki, E. Rachlew-Källne, G. Sundström, and M. Kirm, Argon 3s autoionization resonances, *Phys. Rev. A* **50**, 1218 (1994).
- [22] J. M. Rost, K. Schulz, M. Domke, and G. Kaindl, Resonance parameters of photo doubly excited helium, *J. Phys. B* **30**, 4663 (1997).
- [23] J. B. West and G. V. Marr, The absolute photoionization cross sections of helium, neon, argon and krypton in the extreme vacuum ultraviolet region of the spectrum, *Proc. R. Soc. A* **349**, 397 (1976).
- [24] G. M. Nikolopoulos and P. Lambropoulos, Effects of free-electron-laser field fluctuations on the frequency response of driven atomic resonances, *Phys. Rev. A* **86**, 033420 (2012).
- [25] L. Aufleger, P. Friebe, P. Rupprecht, A. Magunia, T. Ding, M. Rebholz, M. Hartmann, V. Stooss, C. Ott, and T. Pfeifer, Pulse length effects on autoionizing states under the influence of intense SASE XUV fields, *J. Phys. B* **53**, 234002 (2020).
- [26] Y. Wang and C. H. Greene, Resonant control of photoelectron directionality by interfering one- and two-photon pathways, *Phys. Rev. A* **103**, 053118 (2021).
- [27] See Supplemental Material at <http://link.aps.org/supplemental/10.1103/PhysRevLett.129.183204> for more details on the influence of coherent  $\omega - 2\omega$  interaction on the PAD.
- [28] S. Li, T. Driver, O. Alexander, B. Cooper, D. Garratt, A. Marinelli, J. P. Cryan, and J. P. Marangos, Time-resolved pump-probe spectroscopy with spectral domain ghost imaging, *Faraday Discuss.* **228**, 488 (2021).